frontiers | Frontiers in Mechanical Engineering

TYPE Original Research
PUBLISHED 07 June 2024
DOI 10.3389/fmech.2024.1406559

OPEN ACCESS

EDITED BY
Kanak Kalita,
Vel Tech Dr. RR & Dr. SR Technical University, India

REVIEWED BY
Lei Li,
Hefei University of Technology, China
Ahmet İPEKÇİ,
Duzce University, Türkiye

*CORRESPONDENCE
Yi Lv,
lvyi202309@163.com

RECEIVED 25 March 2024
ACCEPTED 21 May 2024
PUBLISHED 07 June 2024

CITATION
Lv Y (2024), Application of image processing technology based on field programmable gate array in mechanical part inspection.
Front. Mech. Eng 10:1406559.
doi: 10.3389/fmech.2024.1406559

Application of image processing technology based on field programmable gate array in mechanical part inspection

Yi Lv*

School of Chemical Engineering and Machinery, Liaodong University, Dandong, China

Introduction: In the field of industrial manufacturing, accurate inspection of mechanical components such as gears and bearings is of Paramount importance. However, the traditional mechanical testing methods are often disturbed by human factors, which not only affects the stability of the test results, but also leads to low efficiency and large error. In order to solve these problems, this research focuses on developing a new edge detection model.

Methods: A novel edge detection model based on field-programmable gate array image processing technology was used in this study. The model uses adaptive threshold multi-directional edge detection technology to identify the edge features of mechanical gears and bearings, aiming at improving the precision of detection.

Results and Discussion: After performance verification, the running time of the model was controlled within 11 s, and the detection error was limited to less than 9%. Compared with the control group and the experimental group, their performance was superior. Further analysis data show that the detection accuracy of this model is as high as 0.9004, its internal resource utilization rate is 88%, and the detection rate is as high as 91%, which are better than the comparison model.

Conclusion: The proposed test model not only significantly improves the efficiency and accuracy of the test, but also fully meets the requirements of the test. This new edge detection model has potential application value in industrial manufacturing field, and provides a new solution for industrial manufacturing quality inspection.

KEYWORDS

FPGA, image processing technology, adaptive threshold, mechanical parts inspection, mechanical gears and bearings

1 Introduction

With the acceleration of the process of industrial modernization, automated production has an increasing demand for accurate detection of mechanical parts, especially mechanical gears and bearing edge profiles (Goli et al., 2021; Zicari et al., 2021). With the trend of standardization and serialization of production, the high quality and precision of mechanical gears and bearings have become the key to ensure product quality and safety (Zhu et al., 2022). Therefore, comprehensive and high-precision detection of key features such as mechanical gears and bearing edges is particularly important in modern industrial production, which is not only related to product quality, but also the cornerstone of improving production efficiency and safe operation of equipment (Lv et al., 2022). Conventional contact detection has gradually been

replaced by non-contact detection based on image processing technology due to its low work efficiency and large errors. This method has high accuracy and strong stability, but it is still difficult to meet the real-time requirements of digital factory systems (Lei, 2022; aponi et al., 2022). Field programmable gate array (FPGA), as a programmable hardware platform, has the advantages of strong parallel computing ability and high flexibility, and has been widely used in image processing technology in the past 20 years. However, through in-depth research and careful design, a new method of using FPGA image processing technology to construct mechanical parts inspection model is proposed in this study. This method makes full use of the parallel computing ability and flexibility of FPGA, and realizes the high-speed and accurate detection of mechanical parts through efficient algorithm design and optimization. The innovation of this research lies in the design and implementation of FPGA-based image processing technology and architecture for the special needs of mechanical parts inspection. This not only improves the real-time and accuracy of the detection system, but also further promotes the development of the manufacturing industry. The research contribution lies in reducing manual errors and resource waste, improving the performance and reliability of detection systems, and promoting the intelligent development of the mechanical manufacturing industry by studying the automation level and efficiency of MPI. The first part of the research is a brief introduction to the application of FPGA and its exploration in the field of mechanical parts by scholars in recent years. The second part provides a detailed introduction to how to use FPGA technology to achieve MPI. The third part analyzes the application effect of the performance testing and detection model of the improved technology. The fourth part is a summary and analysis of the research results.

2 Related works

With the progress of computer technology and electronic technology, various instruments have developed towards intelligence, miniaturization, and multifunctional directions. FPGA technology can help implement various digital logic. In recent years, many scholars have conducted research on it. Wang's team proposed the use of acoustic resonance frequency tracking technology, which is implemented by FPGA devices, to address the issue of low detection ability of non-invasive medical oxygen sensors. Comparative experiments have shown that the sensitivity limit of this method is 1000 ppm, the response time is 4 s, and it has detection capability in a wide concentration range of 1000 ppm to 100% (Wang et al., 2022). In order to improve the encryption effect of voice messages, Kumar et al. Proposed an encryption method based on lightweight AES algorithm and FPGA technology. Simulation analysis of the encryption method showed that, The method has a significantly better encryption effect than traditional methods and is highly practical (Kumar et al., 2022). Scholars such as Cambridge proposed a stereo vision system based on semi global matching and FPGA to address the issue of low real-time generation of dense and robust disparity maps in many video processing applications. The frame rate for disparity map processing in this system is 25FPS, with 256 disparity levels, and excellent memory utilization, processing performance, and accuracy (Cambuim et al., 2020). Pham-Quoc et al. proposed a system based on convolutional neural network model and FPGA technology to address the computational difficulty of image processing in artificial intelligence applications. Empirical analysis shows that the system can work at 159 MHz, and its power consumption is only 3.179 W, which is suitable for edge computing applications (Pham-Quoc et al., 2022). Brunella and other researchers proposed the use of FPGA software to address the expansion issue of universal central processing unit technology in modern computer network interface cards. Comparative experiments have shown that the proposed method can run dynamically loaded programs, achieve packet processing throughput of high-end CPU cores, and provide a 10 times lower packet forwarding latency (Brunella et al., 2022).

With the rapid progress of science and technology, the mechanical industry is facing digital transformation. To adapt to this change, machinery is also gradually updating and upgrading based on automation technology. Every component in machinery is very important, and scholars are exploring this field. For example, Roy et al. proposed a process detection system that utilizes automatic fiber placement machines and optical coherence tomography technology to address the complex quality control process of traditional manufacturing parts. This detection system can analyze differences to detect manufacturing anomalies and minimize process variability (Kumar et al., 2022). Yang's team proposed a construction orientation experiment based on the orientation relationship between force and layer to address the issue of whether parts manufactured by stereo lithography exhibit anisotropy. In all construction directions, whether it is planar construction or edge construction, there are significant differences in the tensile strength of the specimens, with a relative range distribution of 35%, indicating that the stereolithographic parts have anisotropy (Yang et al., 2021). Cica's team proposed a milling based processing strategy for the wall thickness and feed rate of thin-walled parts to address the issue of the impact of process parameter selection on the quality of processed products. This strategy can synchronously optimize the machining parameters of thin-walled parts during the machining process (Cica et al., 2020). Yang et al. proposed a new process control method to improve the reusability of polyamide 12 powder in response to the high economic losses and environmental friendliness of selective laser sintering additive manufacturing of complex parts. The results indicate that this method can produce printed samples with high tensile strength of 18.04% and high elongation at break of 55.29% (Yang et al., 2020). Zheng et al. proposed a method for simulating weathering layer metal welding using solar processing technology under environmental conditions to address the issue of energy waste during the welding process of metal parts. This method can provide new ideas for astronaut assisted maintenance and manufacturing in subsequent lunar and Martian missions (Zheng and Qiao, 2020).

In summary, FPGA technology has made contributions in many fields, and many high-tech technologies have been applied in the field of mechanical parts. However, there is still little research that will combine the two at present. Therefore, this study will combine the two to explore potential research value and fill the research gap in this field.

3 MPI based on FPGA image processing technology

Traditional non-contact detection based on image processing technology has problems such as poor real-time performance. Based

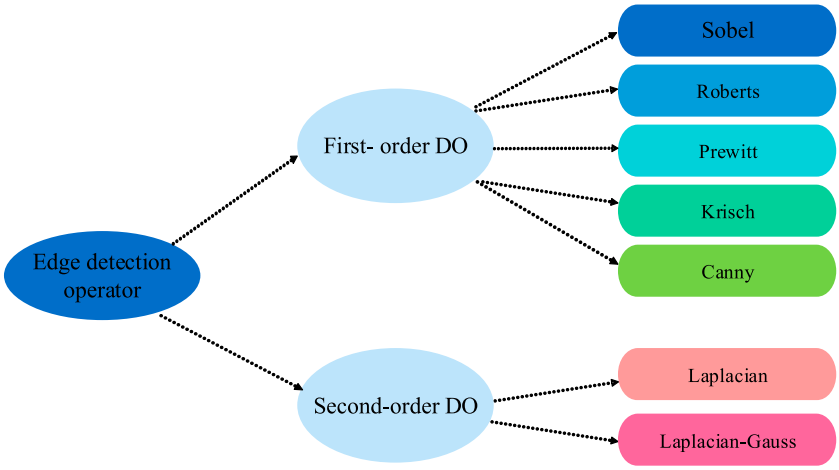

FIGURE 1
Classification plot of the edge detection algorithm.

on this background, this chapter will introduce how to use adaptive threshold (AT) based multi-directional part edge detection (MD-PED) technology combined with FPGA technology to construct an MPI model.

3.1 MD-PED technology based on adaptive threshold

In non-contact detection of mechanical parts, edge detection is a fundamental issue in image processing technology. The purpose of edge detection is to identify points in digital images with significant brightness changes. Image edge detection significantly reduces the amount of data and eliminates information that can be considered irrelevant, preserving important structural attributes of the image. Therefore, edge detection plays a very important role in image processing. The characteristics of the algorithm will directly affect the performance of the MPI system. Edge detection algorithms can be divided into two types: first-order differential operator (DO) and second-order DO. The specific algorithm classification is shown in Figure 1 (Dhillon and Chouhan, 2022).

In Figure 1, edge detection operators based on first-order differentiation include Sobel, Roberts, Prewitt, Krisch, and Canny. This type of operator utilizes the extreme value method of detecting gradient amplitude to extract boundaries. In the algorithm implementation process, 2 * 2 or 3 * 3 operator templates are used as convolution kernels to perform convolution sum operations on each pixel in the original image, and then appropriate thresholds are selected for threshold judgment to extract edges. The Canny operator is a new edge detection operator proposed on the basis of summarizing traditional operators such as Robert, Prewitt, and Sobel, which are sensitive to noise and have low edge positioning accuracy. The edge detection operators based on second-order differentiation include Laplacian and Laplacian Gauss. This type of operator utilizes the principle of second-order differential zero crossing to extract boundary points. The Sobel operator has the advantages of simple and easy implementation, high efficiency and speed, low noise interference, multi-directionality, applicability to grayscale and color images, and adjustable parameters. Therefore, Sobel is most commonly used in non-contact testing of mechanical parts. The traditional Sobel algorithm (tSO) carries out convolution calculations on discrete pixels in the original image. It can separately calculate the image's edge information in the horizontal and perpendicular directions, thereby generating continuous edge information and better depicting the boundaries of the object. The convolution calculation is shown in Eqs 1, 2 (Xu et al., 2022).

$$G_x = \begin{bmatrix} -1 & 0 & 1 \\ -2 & 0 & 2 \\ -1 & 0 & 1 \end{bmatrix} * f \tag{1}$$

In Eq. 1, f represents the original image. G_x represents the convolutional calculation result between the horizontal convolution kernel and the 3 * 3 neighborhood of the original image.

$$G_y = \begin{bmatrix} -1 & -2 & -1 \\ 0 & 0 & 0 \\ 1 & 2 & 1 \end{bmatrix} * f \tag{2}$$

In Eq. 2, G_y represents the same as G_x but in the perpendicular kernel. If the original image is $f(i, j)$, the gradient calculation in the horizontal and vertical directions is Eqs 3, 4.

$$|G_x| = |f(i-1, j+1) + 2f(i, j+1) + \cdots - 2f(i, j-1) - f(i+1, j-1)| \tag{3}$$

In Eq. 3, $|G_x|$ represents the convolutional gradient value in the horizontal direction.

$$|G_y| = |f(i+1, j-1) + 2f(i+1, j) + \cdots - 2f(i-1, j) - f(i-1, j+1)| \tag{4}$$

In Eq. 4, $|G_y|$ represents the convolutional gradient value in the vertical direction. The final output result takes the maximum value of this point, as shown in Eq. 5.

$$G = \max\left(|G_x|, |G_y|\right) \tag{5}$$

In Eq. 5, the final extreme value G is compared with the set threshold to determine the edge of the image. However, there are

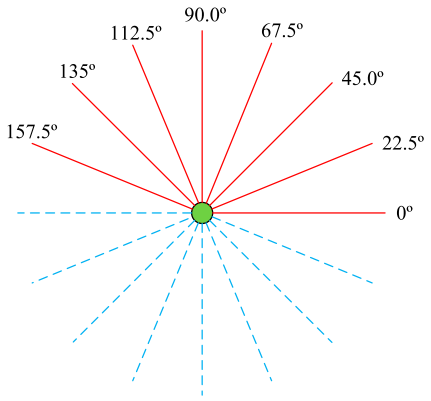

FIGURE 2
Extension template in eight directions.

many edge directions in the actual image, and using only two direction templates cannot detect other gradient directions, which may miss out on a lot of edge information. Therefore, to overcome the drawbacks of tSO in border detection and add marginal information from other orientations, this study extends the tSO template and uses an extended multi-directional template operator for detecting edge. Expanding templates in multiple directions is Figure 2.

In Figure 2, solid lines represent the eight improved directions, while dashed lines represent their symmetrical directions. The Sobel detection operator performs convolution calculations on these eight directions, and the final output extremum calculation is Eq. 6.

$$G' = \max\left(|G_0|, |G_{22.5}|, |G_{45}|, |G_{67.5}|, |G_{90}|, |G_{112.5}|, |G_{135}|, |G_{157.5}|\right) \tag{6}$$

In Eq. 6, G_0, $G_{22.5}$, G_{45}, $G_{67.5}$, G_{90}, $G_{112.5}$, G_{135}, and $G_{175.5}$ respectively represent the convolution calculation results in eight directions. Finally, to compare the extreme value G' to the set threshold to determine the image edge. Expanding in eight directions can improve the detection integrity of Sobel detection operators, but it cannot eliminate the impact of noise points on their accuracy. Therefore, it is proposed to reduce the impact of noise points on edge detection by changing the threshold. But traditional manual threshold setting has a large error. To choose a rational threshold and reduce human error in threshold selection, this study proposes a simple and resultful threshold adaptive algorithm. The image will be segmented into plentiful pixel windows in the form of a 3 * 3 matrix, and the median of the pixel grayscale within the 3 * 3 window will be promptly calculated as an AT. The process is Figure 3.

In Figure 3, sort the grayscale of pixels within the 3 * 3 window by row, selecting the max, median, and min values. Select the min-max values, the max of the min values, and the intermediate value of the median from the obtained maximum, median, and minimum values. Finally, select the median of the three values as the adaptive threshold to achieve MD-PED technology with AT.

3.2 Design of MPI model for image processing technology based on FPGA

Although the MD-PED grounded on ATs can accurately detect images from multiple directions. However, in practical industrial testing, using software based serial processing is difficult to meet the real-time requirements of the system. FPGA is a programmable logic device used to implement hardware functions of digital circuits. FPGA consists of an interconnected logic gate array and a large number of programmable logic elements, such as programmable logic units, lookup tables, etc. It allows users to configure and reprogram hardware logic based on specific application requirements. Compared with application specific integrated circuits, FPGA has higher flexibility and reconfigurability. FPGA is suitable for applications in many fields, including digital signal processing, image processing, communication, embedded systems, and scientific computing. It has advantages such as high performance, low power consumption, low cost, and fast launch, making it very suitable for applications that require customized hardware functions. Therefore, this study proposes to use FPGA technology to construct an MPI model to improve the accuracy and real-time performance of mechanical inspection. The main process of image processing using FPGA technology is Figure 4 (Zhang et al., 2023).

In Figure 4, the image data obtained by the camera first needs to undergo image preprocessing through two processes: image acquisition and grayscale conversion. After preprocessing the image data, the image edge is obtained by adaptive selection of edge detection threshold and edge computing. Afterwards, binary processing is performed, and finally, the binary edge image is output to the analog signal display device for real-time edge display. The conversion relationship of grayscale images is Eq. 7.

$$g(i,j) = 0.299^{*}R(i,j) + 0.587^{*}G(i,j) + 0.114^{*}B(i,j) \tag{7}$$

In Eq. 7, $g(i,j)$ represents the grayscale value after conversion. $R(i,j)$, $G(i,j)$ and $B(i,j)$ represent the three components of the color image in the color model, respectively. To avoid low-speed floating-point operations, optimize time (7) as shown in Eq. 8.

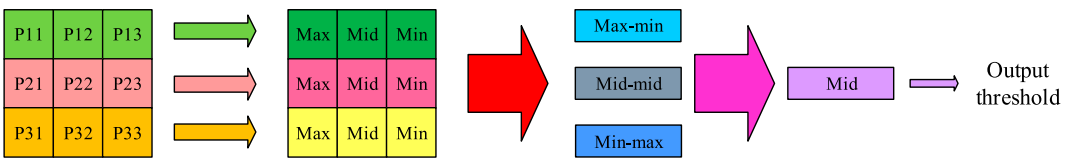

FIGURE 3
Workflow of the threshold-adaptive algorithm.

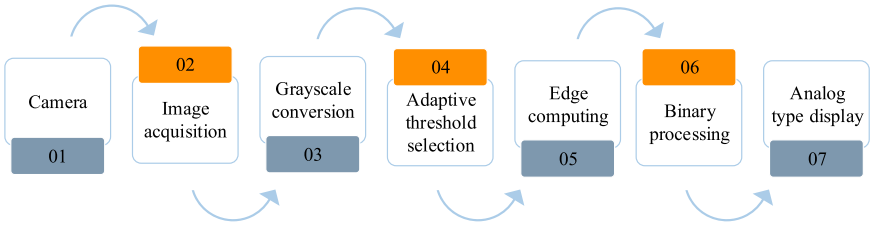

FIGURE 4
Image processing process based on FPGA technology.

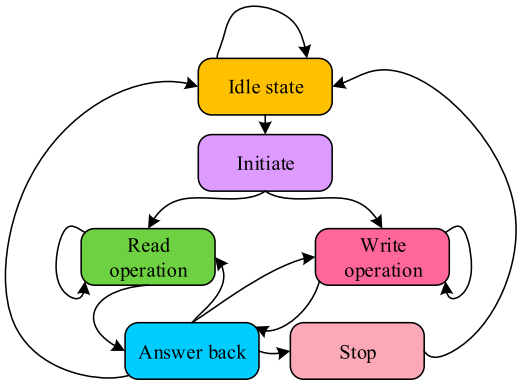

FIGURE 5
The data transfer state transfer diagram.

$$g(i,j) = (76*R(i,j) + 150*G(i,j) + 30*B(i,j))/256 \quad (8)$$

However, using division operation in Eq. 8 will consume a large amount of hardware resources when implementing FPGA technology. Therefore, it is necessary to replace the division operation with a left shift operation. Firstly, convert the computational equation into an inequality, as shown in Eq. 9.

$$g(i,j) = (76*R(i,j) + 150*G(i,j) + 30*B(i,j)) \gg 8 \quad (9)$$

According to the inequality, the three components of the new color image are obtained, and the first component is Eq. 10.

$$R_1(i,j) = 76*R(i,j) = (R(i,j) \ll 6) + (R(i,j) \ll 3) + (R(i,j) \ll 2) \quad (10)$$

The second component is Eq. 11.

$$G_2(i,j) = 150*G(i,j) \quad (11)$$

The third component is Eq. 12.

$$B_2(i,j) = 30*B(i,j) = (B(i,j) \ll 5) - (B(i,j) \ll 1) \quad (12)$$

According to the three components of the newly obtained color image, calculate the grayscale value as shown in Eq. 13.

$$g(i,j) = (R_2(i,j) + G_2(i,j) + B_2(i,j)) \gg 8 \quad (13)$$

By converting the calculation formula, the computational speed of grayscale conversion can be improved to meet the real-time requirements of image processing. When using FPGA technology for image processing, the data transmission process is very important. The various state transitions involved in the transmission process are achieved through a finite synchronous state machine, as shown in Figure 5.

In Figure 5, at the beginning, the bus is in an idle state, and after the FPGA issues a bus request, it enters the startup state. Under the initial conditions, read and write requests are detected, and when the read request is at high level, the next condition enters the read working condition. If the write request is high, the next state will jump to the write working state. In the read and write states, if the transfer bytes are less than 8 bits, the read and write operations will continue. If the transmission reaches 8 bits, it will enter the reply state. In the response state, when the control device responds effectively, it enters the read or write working state and continues to transmit data one byte after another. If the response is invalid, the next state will jump to the paused state. In the case of a stop, if the termination condition is reached, it indicates that the data transmission has ended, and the subsequent state will enter an idle state, thereby relieving the constraints of the bus. Through this transmission process, data loss can be reduced and detection accuracy can be improved. In summary, the MPI model structure based on FPGA image processing technology is Figure 6.

In Figure 6, the MPI model mainly consists of a mechanical control part, a camera, FPGA based image processing, and an analog signal display part. The mechanical control part of the system mainly plays a role in controlling the movement of the camera and carrying the parts to be tested, so as to align the camera with the tested parts and complete the collection of part images. The image processing part based on FPGA preprocesses and edge detects the collected images, and finally displays the edge detection results in real-time through a simulated display.

4 Performance testing of improved technology and analysis of MPI model effectiveness

To verify the performance of the proposed MD-PED technology based on AT and the effectiveness of the MPI model using FPGA image processing technology, comparative experiments are conducted in this study.

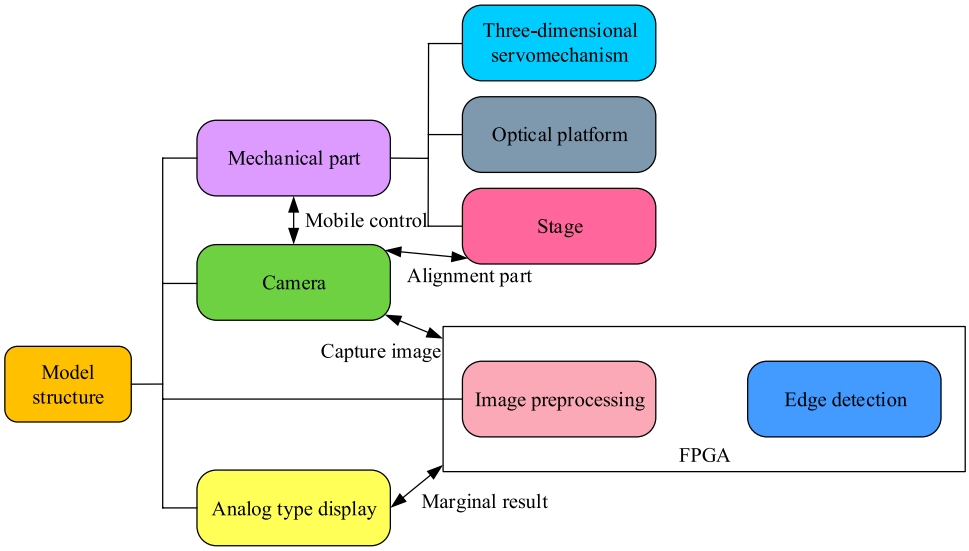

FIGURE 6
Schematic diagram of the detection model structure of the mechanical parts.

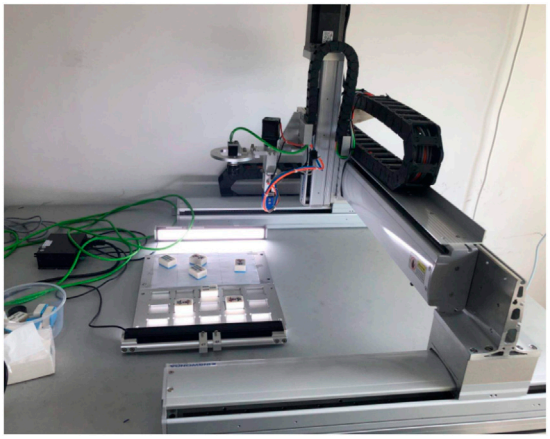

FIGURE 7
Figure of the completed test and detection device.

4.1 Performance comparison testing for improved detection techniques

The experiment is conducted using a 3D servo platform, precision optical platform, camera, stage, and other devices to build the experimental platform. After completion, it is shown in Figure 7.

After setting up the test platform, ensure that all equipment is securely connected and necessary calibration is carried out. Then download the DAGM 2007 dataset and use it as the trial dataset. The DAGM 2007 dataset is an industrial light surface defect recognition dataset published by the Heidelberg Image Processing Collaboration Center in Germany, which contains 10 categories with a total of 10,000 images. The first six classes are development sets, and the last four classes are competition sets. The development dataset for each category contains 1,000 “no defect” images and 150 “defective” images. Each category in the competition dataset contains 2,000 “free” images and 300 “defective” images. A “defect-free” image shows a background texture without defects, while a “defect-free” image has exactly one marked defect on the background texture. Then, for each image in the data set, the necessary pre-processing is carried out, such as grayscale, denoising, contrast enhancement, etc., to improve the image quality. Sobel edge detection technology, Roberts edge detection technology and Prewitt edge detection technology were selected as the control group. And for each edge detection technology, we write or apply a ready-made algorithm to process the image. Record the edge images detected by each technique and save the results. Next, the mechanical gear and bearing are placed on the platform, and the image is captured using the built test platform, and the captured image is processed by the above three edge detection technologies. The performance of different edge detection technologies in the detection degree, detection time and error of part edge image was compared by calculating the evaluation indexes such as the detection degree, detection time and error of part edge image. The test results of mechanical gears and bearings are shown in Figure 8.

In Figure 8, after using different detection techniques to detect gears and bearings in machinery, Sobel, Roberts, and Prewitt techniques have low recognition, many breakpoints, and a lack of internal details for multi edge MPI. The improved technology has a higher detection effect on gears and bearings than the control experimental group, and the continuity of the detection results is good, presenting more details. At the same time, the internal edge contour information of the part is also presented in detail, making the internal and external edge contour information of the part more complete. Compare the detection time and error of the four technologies, and the experimental results are shown in Figure 9.

In Figure 9A, the MPI times for Sobel, Roberts, Prewitt, and improved technology are 19 s, 18 s, 18 s, and 11 s, respectively. The detection time of the improved technology is shorter than that of the

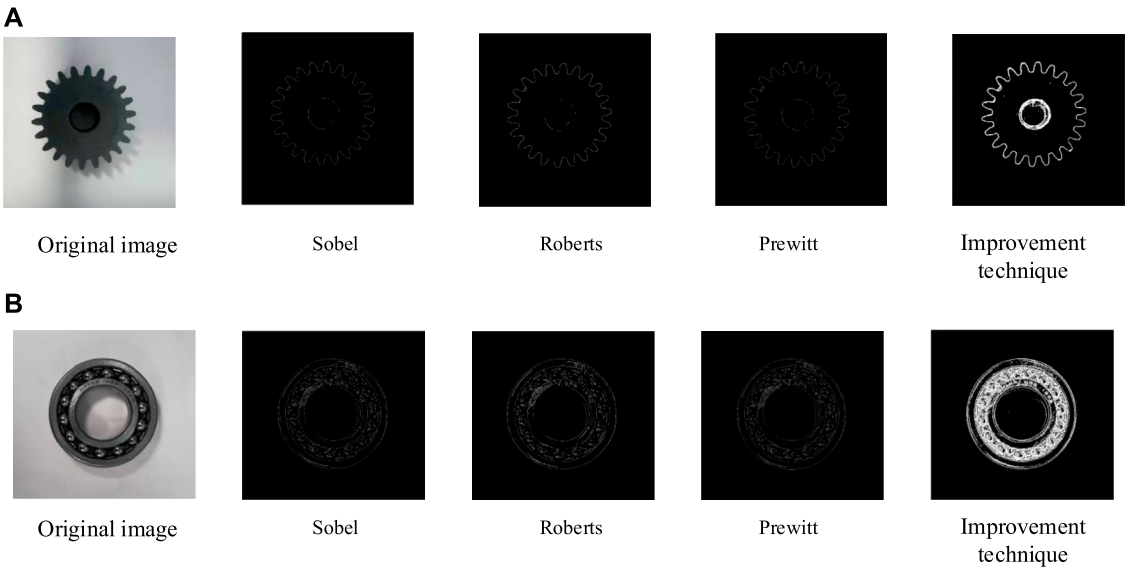

FIGURE 8
The testing results of mechanical gear and bearing under Sobel, Robert, Prewitt and research are presented. **(A)** The testing results of mechanical gear under Sobel, Robert, Prewitt and research are presented. **(B)** The testing results of bearing under Sobel, Robert, Prewitt and research are presented.

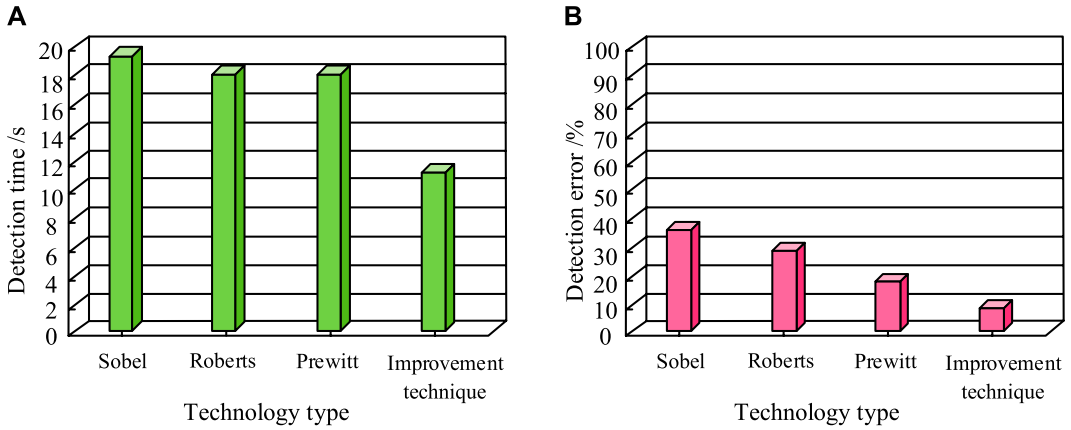

FIGURE 9
Detection time and error. **(A)** Detection time. **(B)** Detection error.

comparative experimental group. In Figure 9B, the MPI errors of the four technologies are 35%, 28%, 18%, and 9%, respectively. The detection error of the improved technology is lower than that of the control group. In summary, the performance of the proposed MD-PED technology built on AT is superior to comparison technology, and it has advantages.

4.2 Analysis of the practical application effect of the proposed MPI model

To verify the actual usage effect of the proposed MPI model based on FPGA technology, Roberts, Prewitt, and improved technology were compared with Matlab software and FPGA hardware to construct MPI models. Using MPI accuracy values, model runtime, internal resource usage during detection, and detection accuracy as evaluation indicators. The test results of standard bolts are shown in Figure 10.

As can be seen from Figure 10, after using different detection techniques to detect standard bolts, the detection effect of the proposed method is higher than that of the comparative detection technique, and the detection results of this method are good in continuity, showing more details. At the same time, the internal edge contour information of the part is also carefully presented, making the internal and external edge contour information of the part more complete. Table 1 is obtained after the accuracy values of six kinds of model testing standard bolts are counted.

In Table 1, the number of edge pixels, number of edge segments, and detection accuracy values are 6,811, 672, and 0.3544 for the Roberts Matlab model, respectively; The Robertst-FPGA model is 7,346, 591, 0.3614; The Prewitt Matlab models

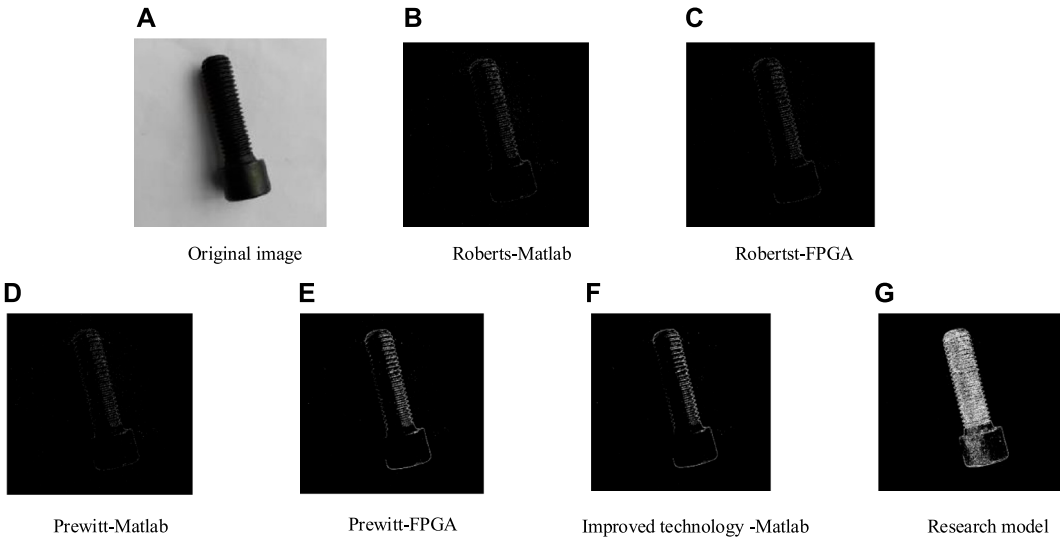

FIGURE 10
Comparison of test results of standard bolts by different methods. **(A)** Original image. **(B)** Roberts-Matlab. **(C)** Robertst-FPGA **(D)** Prewitt-Matlab. **(E)** Prewitt-FPGA **(F)** Improved technology -Matlab. **(G)** Research model.

TABLE 1 Accuracy value of standard bolt detection without detection model.

Serial number	Model class	Number of edge pixels	Number of edge segments	Detection accuracy value
1	Roberts-Matlab	6,811	714	0.3544
2	Robertst-FPGA	7,346	591	0.3614
3	Prewitt-Matlab	8,811	701	0.4102
4	Prewitt-FPGA	17,854	314	0.6471
5	Improved technology -Matlab	20,647	492	0.8014
6	Research model	76,148	497	0.9004

are 8,811, 701, 0.4102; The Prewitt-FPGA model is 17,854, 314, 0.6471; The improved technology-Matlab models are 20,647, 492, and 0.8014; The research models are 76,148, 497, and 0.9004. The data shows that the research model has the largest number of edge pixels, fewer edge segments, and high detection accuracy values, indicating that it can detect more detailed features in standard bolts with higher accuracy than the comparative model. The running time results of six models for detecting standard gears, bearings, and bolts are shown in Figure 11.

In Figure 11, when testing the standard gear, the usage time of Roberts Matlab, Robertst FPGA, Prewitt Matlab, Prewitt FPGA, Improved Technology-Matlab, and the research model were 1,550 ms, 21 ms, 3,601 ms, 21 ms, 10,411 ms, and 21 ms, respectively. When testing standard bolts, the usage time of the six models is 460 ms, 18 ms, 2,531 ms, 18 ms, 10,314 ms, and 18 ms. When testing standard bearings, the usage time of each model is 970 ms, 17 ms, 2,577 ms, 17 ms, 8,351 ms, 17 ms. The above results show that the mechanical detection model built with FPGA technology does show significant advantages in detection time, but it has not reached the speed in large-scale production lines, so in the future, it can be considered to combine FPGA technology with other advanced technologies to further improve the comprehensive performance of the detection system. Statistical analysis was conducted on the internal resource occupancy and detection accuracy of six models during detection, and the experimental results are shown in Figure 12.

In Figure 12, the internal resource occupancy rate and detection accuracy rate of Roberts Matlab are 51% and 65%, respectively; Robertst-FPGA was 73% and 76%, respectively; Prewitt Matlab was 62% and 68% respectively; The Prewitt-FPGA model is 73%, 76%; 78% and 68% for Improved Technology Matla; The research models were 88% and 91%, respectively. The data proves that the research model has the highest internal resource occupancy rate, indicating that the model has fast computational speed and can improve the real-time performance of MPI. At the same time, the detection accuracy of this model is also the highest, superior to the comparison model. In summary, the proposed FPGA based

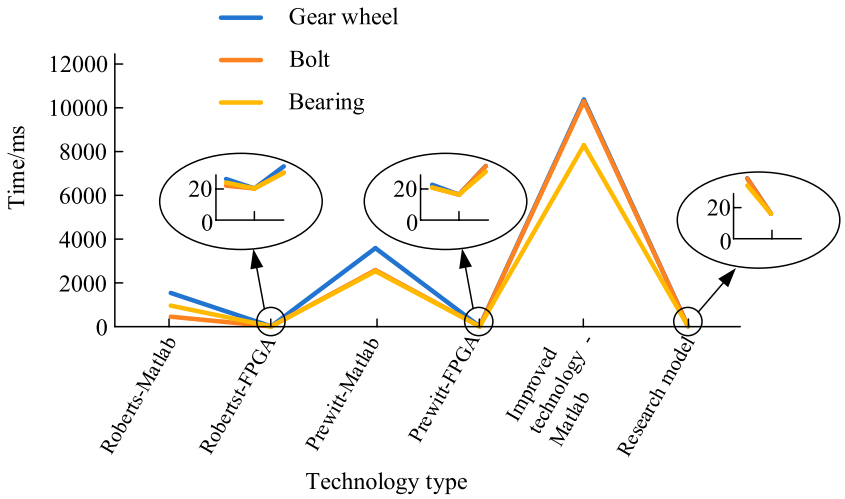

FIGURE 11
Running time of standard gears, bearings and bolts in six models.

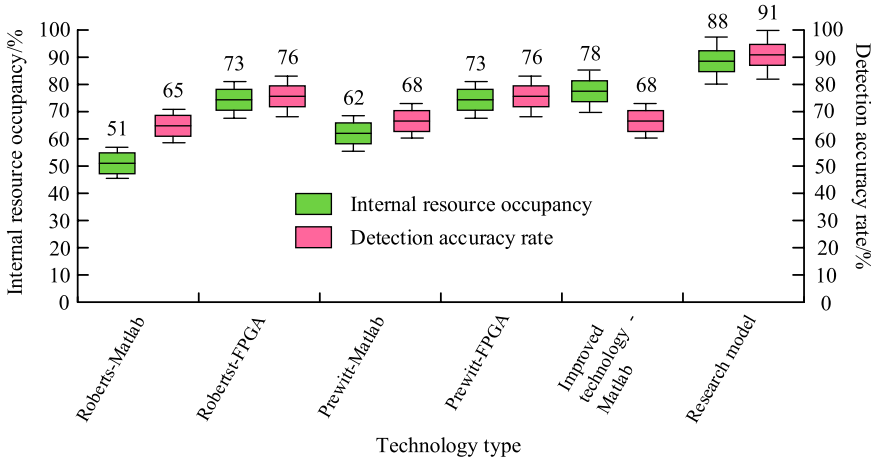

FIGURE 12
Model Internal resource occupancy and detection accuracy.

image processing technology has the best performance in the use of mechanical component inspection models.

5 Conclusion

The development of mechanical manufacturing technology has increasingly high requirements for the quality of mechanical parts. The traditional MPI method has the problems of unstable manual operation, low efficiency, and error prone. In response to this, this study improved the MD-PED technology through ATs, and constructed an MPI model using FPGA image processing technology. Subsequently, comparative experiments were conducted on the improved technology. The results showed that the improved technology had good continuity in the detection results, presented more details, and had a running time of 11 s and a detection error of 9%, both lower than the comparative experimental group. The results of verifying the effectiveness of the proposed MPI model showed that the detection accuracy, internal resource utilization, and detection accuracy of the model were 0.9004, 88%, and 91%, respectively, which are higher than the comparison model. At the same time, the detection times of the model were 21 ms, 18 ms, and 17 ms, all lower than those of the comparative model. In summary, the proposed MPI model combining AT-based MD-PED technology with FPGA image processing technology could improve the accuracy of mechanical inspection and meet real-time requirements, as well as improve the quality control level of mechanical inspection. While the study's proposed approach performs well in many ways, it still has some limitations to consider. First of all, the method is based on the edge characteristics of the part for detection, so when the size or

shape of the part changes significantly, it may be necessary to readjust and optimize the detection parameters to ensure the accuracy and efficiency of the detection. Therefore, this method may face challenges when dealing with mechanical parts with large differences in size and features. Second, while the image processing technology of FPgas increases the speed of detection, it also increases the consumption of internal resources, which can be a limiting factor when processing large or high-resolution images. In addition, the performance of this method is greatly affected by the image quality. If the input image quality is poor, such as noise, blurring and other problems, the accuracy of edge detection will be affected. Finally, although the method shows high detection accuracy and efficiency in the experiment, it fails to meet the requirements of large-scale application in industry, and there are still many indicators that are not compared. A more comprehensive evaluation is needed in the future to ensure that it can meet the demanding requirements of industrial applications.

Data availability statement

The original contributions presented in the study are included in the article/Supplementary material, further inquiries can be directed to the corresponding author.

Author contributions

YL: Writing–original draft, Writing–review and editing.

Funding

The author(s) declare that no financial support was received for the research, authorship, and/or publication of this article.

Conflict of interest

The author declares that the research was conducted in the absence of any commercial or financial relationships that could be construed as a potential conflict of interest.

Publisher's note

References

aponi, S., Passeri, A., Capponi, G., Fioretto, D., Vassalli, M., and Mattarelli, M. (2022). Non-contact elastography methods in mechanobiology: a point of view. *Eur. Biophysics J.* 51 (2), 99–104. doi:10.1007/s00249-021-01567-9

Brunella, M., Belocchi, G., Bonola, M., Pontarelli, S., Siracusano, G., Bianchi, G., et al. (2022). hXDP: efficient software packet processing on FPGA NICs. *Commun. ACM* 65 (8), 92–100. doi:10.1145/3543668

Cambuim, L., Oliveira, L., Barros, E., and Ferreira, A. (2020). An FPGA-based real-time occlusion robust stereo vision system using semi-global matching. *J. Real-Time Image Process.* 17 (5), 1447–1468. doi:10.1007/s11554-019-00902-w

Cica, D., Borojevic, S., Joti, G., Sredanovic, B., and Tesic, S. (2020). Multiple performance characteristics optimization in end milling of thin-walled parts using desirability function. *Trans. Can. Soc. Mech. Eng.* 44 (1), 84–94. doi:10.1139/tcsme-2019-0038

Dhillon, D., and Chouhan, R. (2022). Enhanced edge detection using SR-Guided threshold maneuvering and window mapping: handling broken edges and noisy structures in canny edges. *IEEE Access* 10 (4), 11191–11205. doi:10.1109/ACCESS.2022.3145428

Goli, A., Tirkolaee, E., and Aydın, N. (2021). Fuzzy integrated cell formation and production scheduling considering automated guided vehicles and human factors. *IEEE Trans. fuzzy Syst.* 29 (12), 3686–3695. doi:10.1109/TFUZZ.2021.3053838

Kumar, K., Ramkumar, K. R., and Kaur, A. (2022). A lightweight AES algorithm implementation for encrypting voice messages using field programmable gate arrays. *J. King Saud. Univ.-Com.* 34 (6), 3878–3885. doi:10.1016/j.jksuci.2020.08.005

Lei, Y. (2022). Research on microvideo character perception and recognition based on target detection technology. *J. Comput. Cognitive Eng.* 1 (2), 83–87. doi:10.47852/bonviewJCCE19522514

Lv, Z., Guo, J., and Lv, H. (2022). Safety poka yoke in zero-defect manufacturing based on digital twins. *IEEE Trans. Industrial Inf.* 19 (2), 1176–1184. doi:10.1109/TII.2021.3139897

Pham-Quoc, C., Nguyen, X., and Thinh, T. (2022). Towards an FPGA-targeted hardware/software co-design framework for CNN-based edge computing. *Mob. Netw. Appl.* 27 (5), 2024–2035. doi:10.1007/s11036-022-01985-9

Wang, J., Chen, M., Chen, Q., and Wang, H. (2022). Medical oxygen sensor based on acoustic resonance frequency tracking using FPGA. *IEEE Sensors J.* 22 (21), 21281–21286. doi:10.1109/JSEN.2022.3208912

Xiong, J., Ye, H., Pei, W., Kong, L., Huo, Q., and Han, Y. (2022). A monitoring and diagnostics method based on FPGA-digital twin for power electronic transformer. *Electr. Power Syst. Res.* 210 (9), 108111–108120. doi:10.1016/j.epsr.2022.108111

Xu, P., Zhou, Z., Shi, H., and Geng, Z. (2022). Anisotropic phase stretch transform-based algorithm for segmentation of activated sludge phase-contrast microscopic image. *IEEE Access* 10 (4), 39518–39532. doi:10.1109/ACCESS.2022.3166603

Yang, F., Jiang, T., Lalier, G., Bartolone, J., and Chen, X. (2020). A process control and interlayer heating approach to reuse polyamide 12 powders and create parts with improved mechanical properties in selective laser sintering. *J. Manuf. Process.* 57 (9), 828–846. doi:10.1016/j.jmapro.2020.07.051

Yang, N., Liu, H., Mi, N., Zhou, Q., He, L., Liu, X., et al. (2021). Anisotropic mechanical properties of rapid prototyping parts fabricated by stereolithography. *Sci. Adv. Mater.* 13 (9), 1812–1819. doi:10.1166/sam.2021.4071

Zhang, T., Rahman, F., Tehranipoor, M., and Farahmandi, F. (2023). FPGA-chain: enabling holistic protection of FPGA supply chain with blockchain technology. *IEEE Des. Test* 40 (2), 127–136. doi:10.1109/MDAT.2022.3213998

Zheng, W., and Qiao, G. (2020). Mechanical behavior of the metal parts welded with extraterrestrial regolith simulant by the solar concentrator in ISRU & ISRF application. *Adv. Space Res.* 65 (10), 2303–2314. doi:10.1016/j.asr.2020.02.008

Zhu, X., Xiong, J., Chen, Y., and Cai, Y. (2022). Safety monitoring of machinery equipment and fault diagnosis method based on support vector machine and improved evidence theory. *Int. J. Inf. Comput. Secur.* 19 (3), 274–287. doi:10.1504/ijics.2022.127133

Zicari, R., Brodersen, J., Brusseau, J., Düdder, B., Eichhorn, T., Ivanov, T., et al. (2021). Z-Inspection®: a process to assess trustworthy ai. *IEEE Trans. Technol. Soc.* 2 (2), 83–97. doi:10.1109/TTS.2021.3066209